IEEE Photonics Journal
An IEEE Photonics Society Publication

Open Access

A Transceiver Design Based on an Autoencoder Network for Multi-Color VLC Systems

Volume 12, Number 3, June 2020

Dong-Fang Zhang
Hong-Yi Yu
Yi-Jun Zhu, *Member, IEEE*
Zhao-Rui Zhu

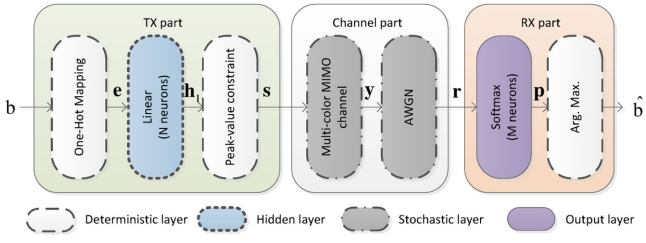

DOI: 10.1109/JPHOT.2020.2990957

A Transceiver Design Based on an Autoencoder Network for Multi-Color VLC Systems

Dong-Fang Zhang, Hong-Yi Yu, Yi-Jun Zhu, *Member, IEEE*, and Zhao-Rui Zhu

National Digital Switching System Engineering and Technological Research Center, Zhengzhou 450000, China

DOI:10.1109/JPHOT.2020.2990957

Manuscript received March 11, 2020; revised April 6, 2020; accepted April 24, 2020. Date of publication April 27, 2020; date of current version May 26, 2020. This work was supported in part by the National Key Research and Development Project under Grant 2018YFB1801903, and in part by the China NSFC under Grants 61671477 and 61901524. Corresponding author: Hong-Yi Yu (e-mail: xxgcmaxyu@163.com).
This article has supplementary downloadable material available at http://ieeexplore.ieee.org, provided by the authors.

Abstract: We propose a transceiver design method based on an autoencoder (AE) network for multi-color visible light communication (VLC) systems. Taking into account the chromaticity constraint described by MacAdam ellipses and the peak-value constraint of transmitted signals, the proposed AE network utilizes a peak-value constraint layer and an integrated loss function which different from previous AE designs. The new structure of AE network can be suitable for VLC systems with different numbers of colors. Additionally, noisy channel state information (CSI) is employed during the training of the AE in order to achieve a better performance for the system with imperfect CSI. After training, a transceiver design with the target of minimizing block error rate (BLER) can be obtained, which simultaneously meets the requirements of lighting. The results of numerical simulation experiments demonstrate that our proposed transceiver design outperforms conventional color shift keying (CSK) constellation design in imperfect CSI channel.

Index Terms: Transceiver design, autoencoder, visible light communication, channel state information, color shift keying.

1. Introduction

Visible light communication (VLC) technology is a communication technology where white light light-emitting diode (LED) can be used as signal transmitter. Based on this, VLC technology provides a new method of wireless communication which is capable of combining lighting and communication together. As a new complementary to wireless communication technology, VLC technology has attracted a large number of academic research in recent years [1]–[6].

The most frequently used LEDs in VLC systems are phosphor-based LED (P-LED) and multi-color LED (e.g., RGB LED and quadrichromatic LED (QLED)). For P-LED, the slow response of the phosphor leads to a limited modulation bandwidth, which is a major challenge in achieving high-speed data transmission [7], [8]. By contrast, when using multi-color LED as the optical source, we can utilize wavelength-division multiplexing (WDM) technology for improving data transmission rate [9]–[12]. What's more, adjustable value of correlated color temperature (CCT) can be achieved

by changing the mixing ratio of multi-color lights, which is another attractive feature of multi-color LED [13]. However, compared with the VLC systems using P-LED, additional considerations about the color of the mixed light transmitted from multi-color LED should be taken for transceiver designs.

In light of this, IEEE 802.15.7 color shift keying (CSK) specially designed for RGB LED is proposed [14]. To meet the requirements of dimming target, CSK in [14] provides a way of mapping a message space onto a color space. With the help of modified billiards algorithms, a method of CSK constellation design for RGB LED is proposed in [15]. In [16], interior point optimization algorithm is utilized to obtain an approximation to the CSK constellation design problem. However, the CSK constellation design problem for QLED is different from that for RGB LED. This is because a set of solutions of mixing ratio of 4-color lights can be obtained for a desired chromaticity coordinate of the mixed light instead of a unique solution in the case of RGB LED [17]. In light of this, a CSK constellation design is proposed with the target of minimizing the minimum pairwise Euclidean distance (MED) [17]. According to ANSI C78.377–2008 [18], a MacAdam ellipse can be used to describe the set of qualified chromaticity coordinates for a desired CCT value, which provides an additional degree of freedom for optimal CSK constellation design. Considering the above factors, a chromaticity-adaptive CSK constellation design is proposed for minimizing the MED of receiving symbols with the assumption of perfect channel state information (CSI) at transmitter [19].

Since the relationship between constellation design and information recovering in multi-color VLC systems is complicated, the optimal solution is difficult to be obtained. As in [17] and [19], iterative methods are utilized to approach the optimal solution. Taking into account the presence of color crosstalk among different color lights and imperfect CSI at transmitter, existing methods of CSK constellation design can not guarantee the best system performance. To handle these shortcomings, deep learning (DL) provides a new means, where the problem of communication system design is considered as an end-to-end reconstruction optimization task from the view of autoencoder (AE) [20]. The new means is a data-driven approach [21], which cares less about the specific form of modulation and treats the communication system as a black box. In particular, for multi-color VLC systems, a transceiver design method based on AE is proposed in [22]. The simulation results in [22] show that AE is capable of automatically learning a transceiver design which achieves a similar performance against the CSK design in [17] for additive white Gaussian noise (AWGN) channel. However, it only considers the case of the fixed mixing ratio of multi-color lights, which only applies to 3-color VLC system.

Following the thought of data-driven approach, we propose a new AE structure which can be used to learn a transceiver design for multi-color VLC systems. Considering the chromaticity constraint described by MacAdam ellipses and the peak-value constraint of transmitted signals, a peak-value constraint layer and a integrated loss function are added to our proposed AE. Under the premise of meeting the requirements in [18], our proposed scheme can be applied to a VLC system with an arbitrary number of colors, which different from [22]. Additionally, channel estimation error is employed during the training of the AE in order to achieve a better performance for the system with imperfect CSI. In simulation experiments, our proposed scheme is compared with two conventional multi-color VLC system, i.e., MIMO-PAM and CSK constellation design in [19]. From numerical results, we can see that AE is capable of automatically finding a solution of transceiver design for multi-color VLC system which owns a similar performance with CSK constellation design with perfect CSI. For the case of imperfect CSI, our proposed scheme provides a better performance than conventional schemes due to that the AE automatically learns the trick of information recovering in imperfect CSI channel, which can not be easily achieved by the conventional design approaches.

The rest of this paper is organized as follows. A multi-color VLC system model is introduced in Section 2. Section 3 provides constraints of transmitted signal in multi-color VLC systems. The transceiver design based on AE is developed in Section 4. Numerical results are presented to illustrate the performance of our proposed scheme in Section 5. Section 6 summarizes this paper.

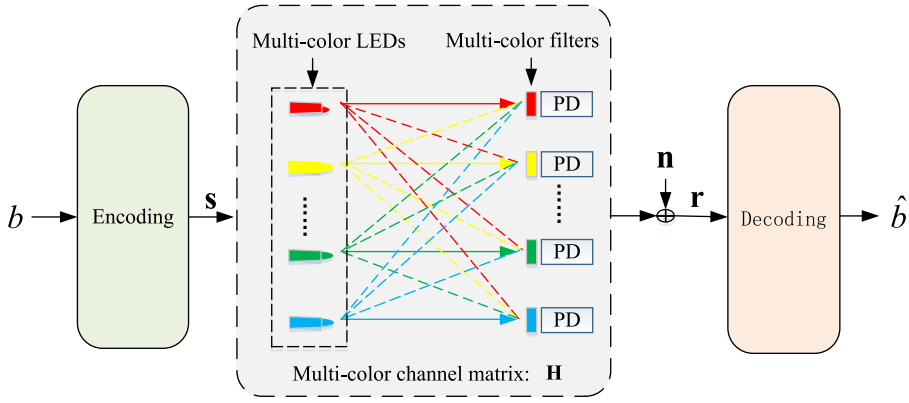

Fig. 1. System model.

2. System Model

Fig. 1 shows a point-to-point multi-color VLC system model. As in Fig. 1, $b \in \mathcal{M} = \{0, 1, \ldots, M\}$ denotes M possible symbols, which are used to transmit $K = \log_2(M)$ bits information. In each time slot, b is mapped into a N-dimensional signal vector $\boldsymbol{s}$, which is used to modulate the optical signal transmitted from a N-color LED. $\boldsymbol{s} \in \mathcal{S} = \{\boldsymbol{s}_1, \boldsymbol{s}_2, \ldots, \boldsymbol{s}_M\}$ and $\mathcal{S} \subseteq \mathbb{R}_+^{N\times 1}$ denotes an N-dimensional constellation. At receiver, a receiving array containing N-color optical filters and N photodiode (PD) receivers are used to transform the optical signal into electrical signal. After the transformation, a decoder is utilized to recover the original information. Stated thus, the N-color VLC system can be seen as a MIMO system with N transmitting antennas and N receiving antennas. A signal-independent AWGN channel is considered in this paper, which is a typical assumption in VLC systems [23]–[28]. Based on the assumption, the N-dimensional received signal vector $\boldsymbol{r}$ can be given as

$$\boldsymbol{r} = \boldsymbol{H} \cdot \boldsymbol{s} + \boldsymbol{n}, \tag{1}$$

where $\boldsymbol{n} \in \mathbb{R}^{N\times 1}$ denotes the noise vector [28], [29]. $\boldsymbol{H} \in \mathbb{R}^{N\times N}$ denotes the N-color MIMO channel matrix. For the N-color channel matrix, let's discuss the case that CSI is perfectly available firstly. As in [5], [30], Lamberts illumination model is used and only the line-of-sight (LOS) part of light signals at receiver is considered in this paper. Unlike the WDM system models in [9]–[12] which assume that there is no color crosstalk at the N-color receiver, we define the N-color channel matrix $\tilde{\boldsymbol{H}} \in \mathbb{R}^{N\times N}$ as:

$$\tilde{\boldsymbol{H}} = \begin{bmatrix} 1-\epsilon & \epsilon & 0 & \cdots & 0 & 0 \\ \epsilon & 1-2\epsilon & \epsilon & \cdots & 0 & 0 \\ \cdots & \cdots & \cdots & \cdots & \cdots & \cdots \\ 0 & 0 & 0 & \cdots & \epsilon & 1-\epsilon \end{bmatrix}, \tag{2}$$

where ϵ denotes the interference ratio [19], [31]. It should be noted that the channel matrix in (2) is based on the assumption that the sizes of both the transmitting array and the receiving array are much smaller than the distance between transmit and receive ends. And without loss of generality, we normalize the channel matrix as in (2). As we known, CSI is not perfectly available in most cases. Here, it is assumed that the VLC system has the estimated CSI $\tilde{\boldsymbol{H}}$ and the channel matrix with the consideration of estimation errors can be given as:

$$\boldsymbol{H} = \tilde{\boldsymbol{H}} + \Delta\boldsymbol{H}, \tag{3}$$

where $\Delta\mathbf{H} \in \mathbb{R}^{N\times N}$ is the channel estimation error [32], [33].

3. Constraints of Transmitted Signal

3.1 Chromaticity Constraint

Chromaticity is a specification which refers to describe the quality of a color. With the help of the CIE 1931 color space chromaticity diagram [34], chromaticity can be represented by chromaticity coordinate (x, y). Let's take RGB LED as the example firstly. The chromaticity coordinate $(\hat{x}, \hat{y})$ of the mixed light emitting from RGB LED can be obtained via the following expression [35]:

$$\begin{bmatrix} \frac{x_r}{y_r} & \frac{x_g}{y_g} & \frac{x_b}{y_b} \\ 1 & 1 & 1 \\ \frac{1-x_r-y_r}{y_r} & \frac{1-x_g-y_g}{y_g} & \frac{1-x_b-y_b}{y_b} \end{bmatrix} \boldsymbol{\rho}_{RGB} = \begin{bmatrix} \frac{\hat{x}}{\hat{y}} \\ 1 \\ \frac{1-\hat{x}-\hat{y}}{\hat{y}} \end{bmatrix}, \tag{4}$$

where (x_c, y_c) denotes the chromaticity coordinates of light transmitted from the c-th color LED chip, where $c \in \{r, g, b\}$. $\boldsymbol{\rho}_{RGB} \in \mathbb{R}^{3\times 1}$ denotes the mixing ratio of the 3-color lights. In order to achieve a desired chromaticity coordinate, we can obtain a unique solution of $\boldsymbol{\rho}_{RGB}$ via solving equations in (4).

For a QLED, we can obtain the chromaticity coordinate of the mixed light as following:

$$\begin{bmatrix} \frac{x_r}{y_r} & \frac{x_a}{y_a} & \frac{x_g}{y_g} & \frac{x_b}{y_b} \\ 1 & 1 & 1 & 1 \\ \frac{1-x_r-y_r}{y_r} & \frac{1-x_a-y_a}{y_a} & \frac{1-x_g-y_g}{y_g} & \frac{1-x_b-y_b}{y_b} \end{bmatrix} \boldsymbol{\rho}_{Q} = \begin{bmatrix} \frac{\hat{x}}{\hat{y}} \\ 1 \\ \frac{1-\hat{x}-\hat{y}}{\hat{y}} \end{bmatrix}, \tag{5}$$

where $\boldsymbol{\rho}_{Q} \in \mathbb{R}^{4\times 1}$ denotes the mixing ratio of the 4-color lights. As we can see from (5), the system of equations is underdetermined due to that there are fewer equations than unknowns. Consequently, for a desired chromaticity coordinate, countless solutions can be obtained via (5). Among all the solutions of (5), we can pick out one or more solutions to achieve the optimal system performance from the point of communication view.

For the sake of clarity, we omit the subscript of $\boldsymbol{\rho}_{RGB}$ and $\boldsymbol{\rho}_{Q}$ and let $\boldsymbol{\rho} \in \mathbb{R}^{N\times 1}$ denote the mixing ratio of the multi-color lights. The relationship between $\boldsymbol{\rho}$ and $\boldsymbol{s}$ is given as following:

$$\mathbb{E}_{\mathcal{S}}[\boldsymbol{s}] \circ \boldsymbol{\eta} = P \cdot \boldsymbol{\rho}, \tag{6}$$

where $\boldsymbol{\eta}$ denotes the coefficient vector of converting luminous flux to forward current. P denotes the total luminous flux. $\mathbb{E}_{\mathcal{S}}[\cdot]$ denotes the statistical expectation over $\mathcal{S}$. $\circ$ denotes Hadamard product.

According to ANSI C78.377–2008 [18], human eyes can not distinguish different colors from each other within a MacAdam ellipse. Consequently, we do not need to fix the chromaticity coordinate of the mixed light at a certain color point in the color space chromaticity diagram. Instead, we can limit the chromaticity coordinate within the ellipse to meet the requirements of lighting, which provides an additional degree of freedom. The chromaticity constraint considering MacAdam ellipse is given as follows:

$$g_{11}(\hat{x} - x_0)^2 + 2g_{12}(\hat{x} - x_0)(\hat{y} - y_0) + g_{22}(\hat{y} - y_0)^2 \leq \xi^2, \tag{7}$$

where g_{11}, g_{12} and g_{22} denote parameters of a ξ-step MacAdam ellipse. (x_0, y_0) denotes the center color point of the ellipse.

3.2 Peak-Value Constraint

In order to protect against destruction of LEDs, the value of all $\boldsymbol{s} \in \mathcal{S}$ should never exceed the current limit of LED [36]. Consequently, the peak-value constraint of $\boldsymbol{s}$ is given as follows:

$$\mathbf{0} \leq \boldsymbol{s} \leq \boldsymbol{I}_{MAX}, \tag{8}$$

where $\boldsymbol{I}_{MAX}$ denotes the limited value.

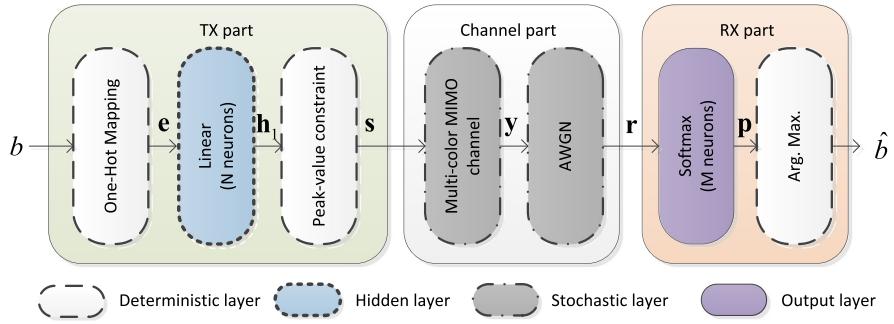

Fig. 2. AE structure.

4. Transceiver Design Based on Autoencoder

As in Fig. 2, the AE structure for multi-color VLC system is showed. The goal of the AE design is to obtain a transceiver design for optimal performance with the consideration on the constraints in (7) and (8). As we can see from Fig. 2, the AE structure includes three parts: transmitter, channel and receiver and we will discuss one by one as following.

4.1 Transmitter

For the i-th training, symbol $b^i \in \mathcal{M}$ is firstly fed into the one-hot mapping layer which outputs $\boldsymbol{e}^i$.

$$\boldsymbol{e}_i(j) = \begin{cases} 0, & j \neq b^i \\ 1, & j = b^i \end{cases}, \tag{9}$$

where $\boldsymbol{e}_i(j)$ denote the j-th element of $\boldsymbol{e}_i$. Via one-hot encoding, the information recovering problem in communication system is converted into a single-label multi-class classification problem, which DL techniques are used to handling. As the dimension of $\boldsymbol{e}^i$ and the output of the transmitter are M and N respectively, a hidden layer with N neurons is employed after the one-hot mapping layer. Besides, linear activation functions are employed in the hidden layer. The output of the hidden layer $\boldsymbol{h}_1^{(i)} \in \mathbb{R}^{N\times 1}$ are given as following:

$$\boldsymbol{h}_1^{(i)} = \boldsymbol{W}_1 \boldsymbol{e}^{(i)} + \boldsymbol{b}_1, \tag{10}$$

where $\boldsymbol{W}_1 \in \mathbb{R}^{N\times M}$ denotes the weight matrix and $\boldsymbol{b}_1 \in \mathbb{R}^{N\times 1}$ denotes the bias vector.

To meet the requirement of the transmitted signal in (8), we use a self-defined peak-value constraint layer as the last layer of the transmitter. Firstly, an exponential linear unit (ELU) is utilized as following:

$$d^{(i)}(j) = f\left(h_1^{(i)}(j)\right) + 1, \tag{11}$$

where $d^{(i)}(j)$ and $h_1^{(i)}(j)$ denote the j-th element of $\boldsymbol{d}^{(i)} \in \mathrm{R}^{N\times 1}$ and $\boldsymbol{h}_1^{(i)}$ respectively. $f(\cdot)$ denotes an ELU, which can be given as following:

$$f(x) = \begin{cases} x, & x \geq 0 \\ \alpha\left(e^x - 1\right), & x < 0 \end{cases}, \tag{12}$$

where $\alpha = 1$. Secondly, we normalize the signal $\boldsymbol{d}^{(i)}$ as following

$$s^{(i)}(j) = I_{MAX}(j) \cdot d^{(i)}(j) / \max_{\tilde{i}} \left(d^{(\tilde{i})}(j)\right), \tag{13}$$

where $I_{MAX}(j)$ and $s^{(i)}(j)$ denote the j-th element of $\boldsymbol{I_{MAX}}$ and $\boldsymbol{s}^{(i)}$ respectively. The equations in (11) and (13) comprise the peak-value constraint layer.

4.2 Channel

Using the channel model in (3), the first layer of the channel part is given as following:

$$\mathbf{y}^{(i)} = \mathbf{H}^{(i)}\mathbf{s}^{(i)} = \left(\tilde{\mathbf{H}} + \Delta\mathbf{H}^{(i)}\right)\mathbf{s}^{(i)}, \tag{14}$$

where the elements of $\Delta\mathbf{H}^{(i)}$ obey the distribution of $\mathcal{N}(0, \sigma_e^2)$ [32], [33]. The second layer is the gaussian noise layer which adds noise to the receiving signal.

$$\mathbf{r}^{(i)} = \mathbf{y}^{(i)} + \mathbf{n}^{(i)}, \tag{15}$$

where $\mathbf{n}^{(i)}$ obeys the distribution of $\mathcal{N}(\mathbf{0}, \sigma_n^2\mathbf{I})$.

4.3 Receiver

In the receiver part, an output layer is included which employ M neurons and softmax activations. The output $\boldsymbol{p}^{(i)} \in \mathbb{R}^{M\times 1}$ is given as following:

$$p^{(i)}(j) = \frac{e^{z^{(i)}(j)}}{\sum_{\tilde{j}}^{M} e^{z^{(i)}(\tilde{j})}}, \tag{16}$$

where $p^{(i)}(j)$ and $z^{(i)}(j)$ denote the j-th element of $\boldsymbol{p}^{(i)}$ and $\boldsymbol{z}^{(i)} \in \mathbb{R}^{M\times 1}$ respectively. $\boldsymbol{z}^{(i)} = \boldsymbol{W}_2\boldsymbol{r}^{(i)} + \boldsymbol{b}_2$. $\boldsymbol{W}_2 \in \mathbb{R}^{M\times N}$ denotes the weight matrix and $\boldsymbol{b}_2 \in \mathbb{R}^{M\times 1}$ denotes the bias vector. As the softmax activation normalize the M inputs into a probability distribution consisting of M probabilities, the estimate of b^j can be obtained by finding the maximum value of $\boldsymbol{p}^{(i)}$.

$$\hat{b}^{(i)} = \arg\max_j \left(p^{(i)}(j)\right). \tag{17}$$

4.4 Cost Function

To achieve a better communication performance along with the consideration on the constraint of transmitted signal in (7), the loss function of the proposed AE is defined as a sum of two parts.

$$L = L_1 + \lambda \cdot L_2, \tag{18}$$

where L_1 denotes the categorial cross-entropy between $\{\boldsymbol{e}^j\}$ and $\{\boldsymbol{p}^j\}$, which corresponding to the aim of minimizing the block error rate (BLER).

$$L_1 = -\frac{1}{m} \cdot \sum_{i=1}^{m} \log\left(p^{(i)}\left(b^{(i)}\right)\right), \tag{19}$$

where m denotes the number of training inputs. In order to meet the constraint in (7), we define L_2 as following:

$$L_2 = g_{11}(\hat{x} - x_0)^2 + 2g_{12}(\hat{x} - x_0)(\hat{y} - y_0) + g_{22}(\hat{y} - y_0)^2. \tag{20}$$

Different from that the arithmetic mean value of $\mathcal{S}$ is used to obtain the mixing ratio of the multi-color lights $\boldsymbol{\rho}$, $\bar{\boldsymbol{\rho}}$ is used instead which is calculated through the statistical average value in the training as following:

$$\bar{\boldsymbol{\rho}} = \frac{1}{P} \cdot \frac{1}{m} \cdot \sum_{i=1}^{m} \boldsymbol{s}^{(i)} \circ \boldsymbol{\eta}. \tag{21}$$

$\lambda > 0$ denotes a relative contribution of L_2 to the overall cost. Based on put L_2 into the calculation of the overall cost, the learning process seeks to minimize the value of L_2 which helps match the constraint in (7). It should be noted that it is not guaranteed that the result of network training will meet the constraint in (7). However, the simple network structure of the AE makes it easy to

TABLE 1
Network Configurations

Layer	Output dimensions	Corresponding equation number
One-hot mapping layer	M	(9)
Dense + linear	N	(10)
Peak-value constraint layer	N	(13)
Multi-color MIMO Channel	N	(14)
AWGN	N	(15)
Dense + softmax	M	(16)
Arg. Max.	1	(17)

converge to a solution within the MacAdam ellipse in (7), which will be verified by a number of simulations in Section 5.

So far, on the base of the cost function and the peak-value constraint layer, the requirements of the transmitted signal in (7) and (8) are considered in the AE design. In (10), (11) and (17), the encoding and decoding operations consist of linear matrix multiplications and additions. The complexity of the transceiver based on AE is $\mathcal{O}(MN)$.

The configurations of the proposed AE are summarized in Table 1. As in Table 1 and Fig. 2, the AE network consists of 7 layers. It should be noted that only 2 of the 7 layers which utilizes linear activations and softmax activations respectively are needed to be optimized during the training process.

As we can see from Fig. 2, the autoencoder in this paper has a unsymmetric structure. The reason is given as follows. Considering using LED as the optical source in the system, the working principle of LED determines that the transmitted signal should be real-valued and nonnegative. To protect LED from being damaged due to overheating, the value of the transmitted signal should never exceed the current limit of LED as in (8). What's more, considering the chromaticity constraint in (7), the statistical expectation of transmitted signal should be limited in a MacAdam ellipse. By contrast, the received signal has no constraint similar to the above [5], [24], [37]. Consequently, an unsymmetric structure is utilized for the autoencoder.

As in Table 1 and Fig. 2, some parts of the proposed AE are designed based on referring to the existing studies on the AE for end-to-end communications in [20], [22], such as the layers expressed by (9), (10), (15), (16) and (17). However, some other parts are different from existing studies. Here, we would make some explanations about the reason for choosing the parameters as following. For loss function, categorial cross-entropy L_1 cooperated with softmax function can obtain a good performance on dealing with a single-label multi-class classification problem. As the messages are one-hot encoded in (9), a good BLER performance of the end-to-end communication system can be achieved via taking categorial cross-entropy as the loss function [20]. As in [20], we define BLER as $\Pr\{\hat{b} \neq b\}$, which is used to measure accuracy of the classification model in this paper. As far as we have known, the chromaticity constraint in (7) can not be directly integrated with any existing AE network. Consequently, we use a self-defined function L_2 in (20) to let the AE network automatically approach to the target of meeting the chromaticity constraint in (7) during the training process. Considering both communication performance and illuminating quality, we define the loss function of our proposed AE as the sum of L_1 and L_2 which is expressed by (18). For the peak-value constraint, the method of normalization used for an average power constraint in [20], [38] can not meet the constraint in (8). And we have tried using the rectified linear unit (ReLU) which has a poor convergence performance under the case that both the categorial cross-entropy L_1 and the self-defined loss function L_2 are considered in this paper. Compared with ReLUs, ELUs have negative values which can fix the dying ReLU problem and is preferable to the fast convergence of the training process [39]. Consequently, ELUs are taken as the activations in the peak-value constraint layer in (8).

To sum up, hyper-parameters of the AE network include the network configurations in Table I, the channel matrix in (2), variances of the estimation error in (14) and the additive noise in (15), the CCT value and the corresponding parameters of MacAdam ellipse, the relative scaling factor

TABLE 2
Parameters of Multi-Color LEDs

	RGB LED (Cree Xlamp MC-E)	RAGB LED (LUMILEDS)
Chromaticity Coordinate		
Red	(0.7006, 0.2993)	(0.6941, 0.3026)
Amber		(0.5979, 0.3995)
Green	(0.1547, 0.8059)	(0.2297, 0.7099)
Blue	(0.1440, 0.0297)	(0.1230, 0.0925)
Luminance Flux - Forward Current Conversion Coefficient		
Red	0.0114 A/lm	0.021 A/lm
Amber		0.014 A/lm
Green	0.0052 A/lm	0.005 A/lm
Blue	0.0427 A/lm	0.015 A/lm

TABLE 3
Parameters of MacAdam Ellipses [18]

CCT	Center point	g_{11}	$2g_{12}$	g_{22}
2700K	(0.459, 0.412)	40×10^4	-39×10^4	28×10^4
5000K	(0.346, 0.359)	56×10^4	-50×10^4	28×10^4
6500K	(0.313, 0.337)	86×10^4	-80×10^4	45×10^4

λ in (18), the current limit of LEDs, the mini-batch size, the learning rate, the number of samples, the generator of random samples and the training environment. For different application scenarios, some hyper-parameters should be tuned. Firstly, the value of K, N and M should be tuned for a specific application scenario. For example, when RGB LED is utilized as the system optical source, N should be set as 3. The values of K and M depend on the number of bits which are desired to be transferred within a time slot. Secondly, the channel matrix in (2) and the variance of the estimation error in (14) should be tuned according to channel situation. Thirdly, the variance of the additive noise in (15) (i.e., SNR) for training should be adjusted according to the values of M and N with engineering experiences. And of course, a two-stage training strategy proposed in [22] can be used here to make the training process more efficient. Fourthly, the current limit of LEDs $\boldsymbol{I}_{MAX}$ should be adjusted according to the datasheet of specific LEDs. Lastly, the CCT value and the parameters of MacAdam ellipse should be tuned according to the illumination requirement in the application scenario. Note that other changes would be made for a broader range of applications of the network design.

5. Numerical Results

Numerical results are presented with the aim of analyzing the performance of proposed transceiver design based on AE in this section. Two kinds of multi-color LEDs are used in this paper whose parameters are listed in Table 2. According to Table 2, two cases are considered in simulations: (1) $N = 3$; (2) $N = 4$. Correspondingly, we let $K = N$ and $M = 2^N$. In simulations, we set ϵ in (2) as 0.1 and assume that the value is the same for each pair of adjacent color channels [19], [31]. As in ANSI C78.377–2008 [18], the step of MacAdam ellipse ξ is set to be 7 and three CCT values are used as in Table 3. Normally, the value of L_1 is expected to be below 0.1 after the training. According to (7) and $\xi = 7$, we set λ to be $1/10^3$ which leads to a proper contribution of L_2 to the overall cost. There is a need to state that the value of λ we set may not be optimal. In order to conform to a custom way of analysing the performance of communication systems, we set $P = 1$ in (6) and use signal-to-noise (SNR) at receiver to illustrate the system performance in this section. The current limit of LEDs in (8) is normalized to one, i.e., $\boldsymbol{I}_{\boldsymbol{MAX}} = [1, 1, \ldots, 1]^T$. For training of the proposed AE, we employ an Adam algorithm [40] with mini-batch size $100 \times M$ and learning rate 0.001. $10^6 \times M$ samples are used for training. During training and testing, the transmitted symbol b^j, the channel estimation error noise vector $\Delta\mathbf{H}^{(i)}$ and the noise vector $\mathbf{n}^{(i)}$ are generated independently from each

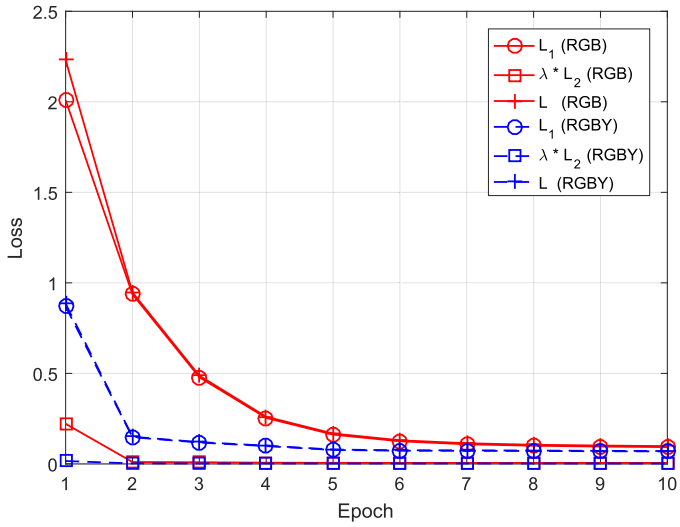

Fig. 3. Convergence performance.

other via using the basic function *random*(·) from the Python Standard Library. In the basic function, the Mersenne Twister is used as the core generator [41]. Note that different random seeds is used for the training and testing stages. The following results of BLERs are obtained via the testing processes, specifically, Monte Carlo simulations. SNR value adopted during the training is set to be 10 (dB). The simulation environment is Python 3.6.2 with TensorFlow 2.0.0 [42].

5.1 Convergence Performance

To illustrate the convergence performance of the proposed AE, we present the relationship between the loss value and the training epoch in training process under the case of perfect CSI. The target CCT value is set as 5700 K here. As in (18), (19) and (20), both the categorial cross-entropy L_1, the self-defined loss function L_2 and the sum of them L are considered in Fig. 3. As in Fig. 3, all of the loss values decrease gradually as the training epochs increase. When the training epoch is bigger than 5, all of the loss values begin to stabilize on a certain value.

5.2 BLER Performance With Perfect CSI

Firstly, let's discuss the perfect CSI case, i.e., $\sigma_e = 0$ in (14). To illustrate the performance of our proposed transceiver design, two other baseline schemes are introduced for comparsion. The first baseline scheme is 2-PAM with maximum likelihood (ML) estimation. Let $\boldsymbol{s}_{PAM} = [s_{PAM,1}, s_{PAM,2}, \ldots, s_{PAM,N}]^T$ denotes the PAM signal vector, where $s_{PAM,i} \in \{0, S_{PAM,i}\}$. The expectation of the PAM signal is $\mathbb{E}[\boldsymbol{s}_{PAM}] = 0.5 \cdot \boldsymbol{S}_{PAM}$, where $\boldsymbol{S}_{PAM} = [S_{PAM,1}, S_{PAM,2}, \ldots, S_{PAM,N}]^T$. For the case that RGB LED is taken as the transmitter, we can obtain the value of $\boldsymbol{S}_{PAM}$ according to (4) and (6). However, countless solutions of $\boldsymbol{S}_{PAM}$ can be obtained via (5) and (6) for the case of RAGB LED. For the convenience of the contrast analysis, $\boldsymbol{S}_{PAM}$ is obtained based on the mixing ratio $\boldsymbol{\rho}$ which is obtained via the proposed scheme. It should be noted that this is not optimal in terms of performance for the first baseline. The second baseline scheme is the multi-color constellation design of CSK which is proposed in [19]. The ML estimation with perfect CSI can be expressed as following:

$$\hat{\boldsymbol{s}} = \arg\min_{\boldsymbol{s}\in\mathcal{S}} \left\{ \left\| \boldsymbol{r} - \tilde{\boldsymbol{H}}\boldsymbol{s} \right\|_2^2 \right\}, \tag{22}$$

where $\hat{\boldsymbol{s}}$ denotes the estimation of $\boldsymbol{s}$ and $\|\cdot\|_2$ denotes the 2-norm. As ML estimation is adopted for both of the two baseline schemes, the complexity of them is $\mathcal{O}(MN)$. Hence, the complexity of

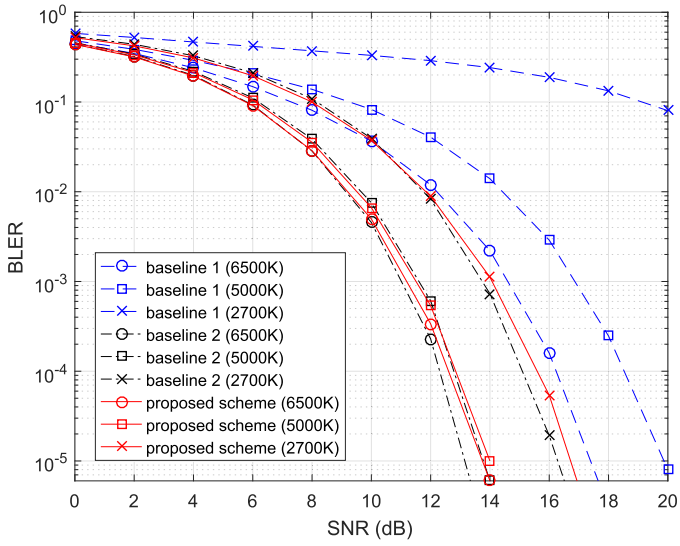

Fig. 4. Performance comparison with different CCT values (RGB).

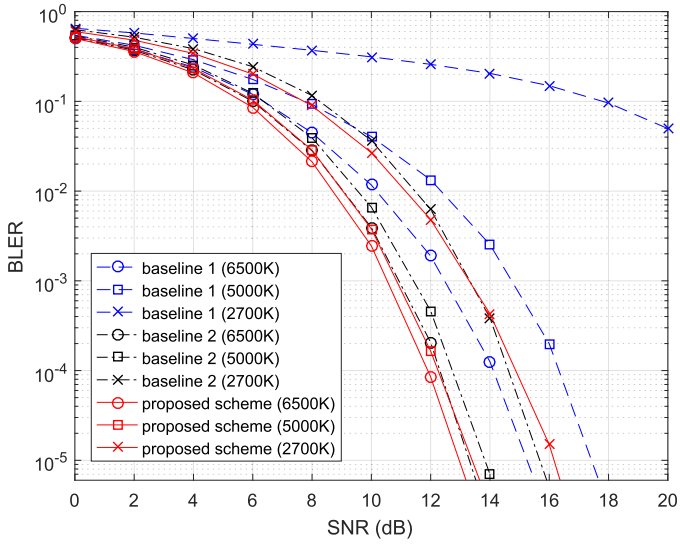

Fig. 5. Performance comparison with different CCT values (RAGB).

the proposed scheme and baseline schemes are at the same magnitude. Fig. 4 and Fig. 5 show the performance comparisons with different CCT values. We can see that the performance of our proposed scheme and the second baseline scheme are similar. And both of them outperform the first baseline scheme for all CCT values. What's more, the performance gaps between different CCT values of the first baseline scheme are much bigger than that of our proposed scheme and the second baseline scheme. In particular, for the case of 2700 K and $SNR < 20\,(dB)$, the BLER is always higher than 10^{-3}. By contrast, our proposed scheme and the second baseline scheme are less sensitive to the changing of CCT values. The reason is that the chromaticity constraint in (7) results in different SNR conditions for different color lights, which leads to decline in performance of both the three schemes. With adequate consideration of the chromaticity constraint, the decline of performance due to the chromaticity constraint in our proposed scheme and the second baseline scheme is relatively small than that in the first scheme.

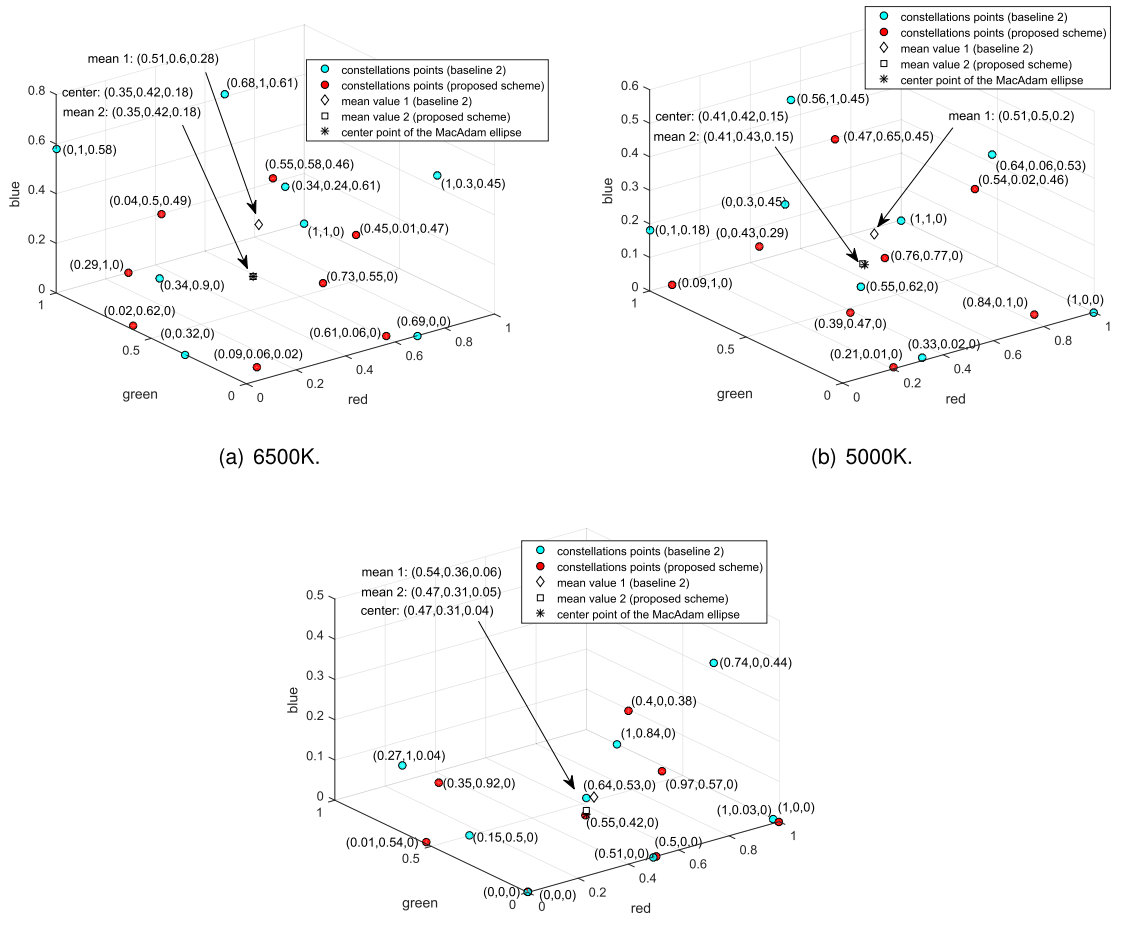

(a) 6500K.

(b) 5000K.

(c) 2700K.

Fig. 6. Generated constellations points of our proposed scheme and the second baseline scheme.

In order to present a more clear comparative analysis of our proposed scheme and the second baseline scheme, constellation points of them are shown in Fig. 6. Considering the convenience of drawings, only the case where we use the RGB LED as the transmitter is presented in Fig. 6. (Other learned constellations used in simulations are presented in Appendix A.) Without loss of generality, all constellation points are assumed to be equiprobable and the mean points in Fig. 6 can be used to obtain the statistical expectation over $\mathcal{S}$. And by calculation, we can obtain that both of the two schemes meet the requirement in (7). From Fig. 6, we can obtain the normalized MEDs of different receiving signals $\boldsymbol{y}$ for our proposed scheme as 1.7612, 1.7036 and 1.2052, where $\boldsymbol{y} = \boldsymbol{H} \cdot \boldsymbol{s}$, $\boldsymbol{s} \in \mathcal{S}$. Similarly, the normalized MEDs of different receiving signals for the second baseline scheme can be obtained as 1.888, 1.745 and 1.4124. The calculation results of the normalized MEDs for the two schemes are similar which are consistent with the BLER performances shown in Fig. 4. The above results show that AE automatically find a solution of the constellation design for the multi-color VLC system which owns a similar performance with CSK constellation design in [19] under the case of perfect CSI.

5.3 BLER Performance With Imperfect CSI

The performance comparisons with the consideration of imperfect CSI are presented in Fig. 7 and Fig. 8. Without loss of generality, 6500 K is set as the target CCT value in the comparisons. For

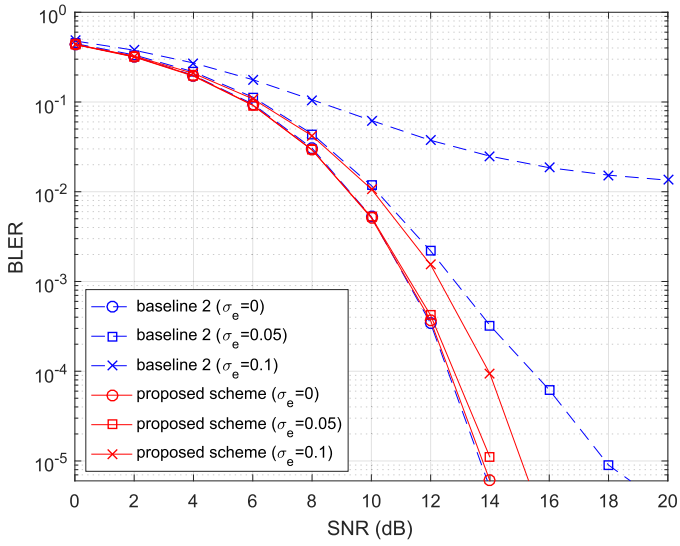

Fig. 7. Performance comparison with imperfect CSI (RGB).

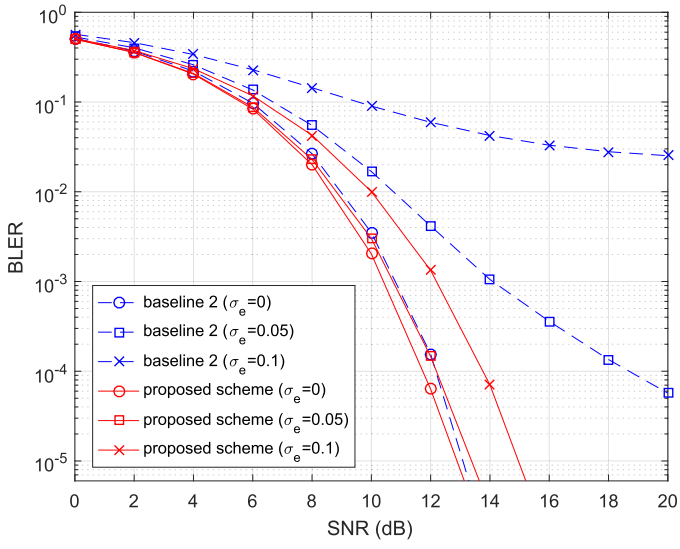

Fig. 8. Performance comparison with imperfect CSI (RAGB).

the second baseline scheme, it must be noted that the ML estimation with imperfect CSI is different from (22) [43], [44], which is given as following:

$$\hat{\boldsymbol{s}} = \arg\min_{\boldsymbol{s}\in\mathcal{S}} \left\{ \frac{\|\boldsymbol{r} - \boldsymbol{H}\boldsymbol{s}\|_2^2}{\sigma_e^2 \|\boldsymbol{s}\|_2^2 + \sigma_n^2} + N \log\left(\sigma_e^2 \|\boldsymbol{s}\|_2^2 + \sigma_n^2\right) \right\}. \tag{23}$$

We can see that our proposed scheme and the second baseline scheme have similar BLER performance under the case of perfect CSI. In contrast, under the case of imperfect CSI, our proposed scheme outperforms the second baseline scheme. What's more, as the standard deviations of the elements of the channel estimation error matrix $\Delta\mathbf{H}$ increase, the BLER performance gap between the two schemes gets bigger. The reason is that the second scheme in [19] considers only the MED of receiving signals, which is not the optimal criteria in the case of imperfect CSI. As far

as we know, there are few publications on constellation design for multi-color VLC systems with imperfect CSI, which is a valuable research issue but beyond the scope of this paper. By contrast with the conventional constellation design method, AE automatically learns the complicated input-output relation with the consideration of imperfect CSI, which helps improving the system performance.

6. Conclusion

In this paper, a transceiver design method based on AE for the multi-color VLC system is proposed. In order to deal with the chromaticity constraint and peak-value constraint, a peak-value constraint layer and a integrated loss function are added to the AE. Under the constraints, AE is able to accomplish the design of constellation generation and detection methods automatically, even under the case where the mixing ratio of different color lights is not unique. Numerical results have shown the AE automatically finds a solution of the constellation design for multi-color VLC systems which owns a similar performance with CSK constellation design in [19] under the case of perfect CSI. The results of simulations also illustrate that the performance of our proposed scheme is better than that of the conventional constellation design scheme under the case of imperfect CSI, for the reason that AE is capable of learning the complicated input-output relation rather than maximizing the MED of receiving signals only. It is noteworthy that the loss function definition in (20) results in that the mean value of the constellation points is close to the center point of the MacAdam ellipse. Consequently, this method does not fully exploit the degree of freedom of constraint region defined by the MacAdam ellipse in (7), which deserves more research in future.

Appendix A
Learned Constellations

This appendix presents the learned constellations for all cases in simulations.

When the CCT value is 6500 K and $\sigma_e = 0$, the learned RGB LED constellation is given by

$$\begin{aligned}\mathcal{S} = \{&[0.0944, 0.0645, 0.0215]^T, [0.4520, 0.0144, 0.4660]^T, [0.0189, 0.6206, 0.0006]^T,\\ &[0.2884, 1.0000, 0.0006]^T, [0.7283, 0.5529, 0.0005]^T, [0.0438, 0.4969, 0.4856]^T,\\ &[0.6094, 0.0580, 0.0016]^T, [0.5497, 0.5799, 0.4595]^T\}\end{aligned}$$

When the CCT value is 5000 K and $\sigma_e = 0$, the learned RGB LED constellation is given by

$$\begin{aligned}\mathcal{S} = \{&[0.0933, 1.0000, 0.0019]^T, [0.7585, 0.7682, 0.0011]^T, [0.2139, 0.0051, 0.0014]^T,\\ &[0.4666, 0.6536, 0.4547]^T, [0.3873, 0.4722, 0.0020]^T, [0.5440, 0.0179, 0.4604]^T,\\ &[0.0045, 0.4276, 0.2932]^T, [0.8422, 0.0996, 0.0028]^T, \}.\end{aligned}$$

When the CCT value is 2700 K and $\sigma_e = 0$, the learned RGB LED constellation is given by

$$\begin{aligned}\mathcal{S} = \{&[0.0100, 0.5400, 0]^T, [0.4000, 0, 0.3800]^T, [0, 0, 0]^T,\\ &[0.9700, 0.5700, 0]^T, [0.5100, 0, 0]^T, [0.5500, 0.4200, 0]^T,\\ &[1.0000, 0, 0]^T, [0.3500, 0.9200, 0]^T\}.\end{aligned}$$

When the CCT value is 6500 K and $\sigma_e = 0$, the learned QLED constellation is given by

$$\begin{aligned}\mathcal{S} = \{&[0.3184, 0.5370, 0.0063, 0.7780]^T, [0.7463, 0.6519, 0.3985, 0.0017]^T,\\ &[0.0107, 0.9075, 0.1414, 0.4095]^T, [0.2417, 0.6381, 0.0090, 0.0074]^T,\\ &[0.9218, 0.0122, 0.5882, 0.1781]^T, [0.3953, 0.0071, 0.5516, 0.0011]^T,\\ &[0.5957, 0.0231, 0.5314, 0.6081]^T, [0.5871, 0.3680, 0.9513, 0.0008]^T,\end{aligned}$$

$$[0.4448, 0.6632, 0.6147, 0.5097]^T, [0.0042, 0.4870, 0.5940, 0.0036]^T,$$
$$[0.3074, 0.0715, 0.0380, 0.3867]^T, [0.6952, 0.1631, 0.0593, 0.0020]^T,$$
$$[0.2658, 0.9502, 0.5646, 0.0009]^T, [0.0107, 0.2917, 0.4471, 0.5171]^T,$$
$$[0.7262, 0.5643, 0.0456, 0.4628]^T, [0.2641, 0.0761, 1.0000, 0.2661]^T\}.$$

When the CCT value is 5000 K and $\sigma_e = 0$, the learned QLED constellation is given by

$$\mathcal{S} = \{[0.0346, 0.5685, 0.0043, 0.0003]^T, [0.5208, 0.0009, 0.5019, 0.0003]^T,$$
$$[0.0030, 0.4815, 0.1670, 0.4879]^T, [0.4792, 0.8868, 0.5119, 0.0003]^T,$$
$$[0.4327, 0.6104, 0.5346, 0.4667]^T, [0.8875, 0.4036, 0.4796, 0.0006]^T,$$
$$[0.5305, 0.6757, 0.0018, 0.0006]^T, [0.1832, 1.0000, 0.0017, 0.3175]^T,$$
$$[0.7526, 0.0826, 0.0025, 0.0006]^T, [0.8464, 0.0124, 0.5251, 0.3844]^T,$$
$$[0.2503, 0.0161, 0.0112, 0.1877]^T, [0.4477, 0.2764, 0.9412, 0.0004]^T,$$
$$[0.0024, 0.7031, 0.5709, 0.0031]^T, [0.3001, 0.0021, 0.6174, 0.4405]^T,$$
$$[0.5537, 0.3984, 0.0029, 0.4817]^T, [0.0050, 0.1043, 0.5776, 0.0007]^T\}.$$

When the CCT value is 2700 K and $\sigma_e = 0$, the learned QLED constellation is given by

$$\mathcal{S} = \{[0.0052, 0.3242, 0.5672, 0.0002]^T, [0.0063, 0.3445, 0.0007, 0]^T,$$
$$[0.4302, 0.4541, 0.4682, 0.0007]^T, [0.6987, 0.0003, 0.0004, 0.0002]^T,$$
$$[0.1737, 1.0000, 0.0003, 0.0001]^T, [0.3461, 0.0001, 0.0005, 0]^T,$$
$$[0.3158, 0.0149, 0.3057, 0.2457]^T, [0.0006, 0.6976, 0.0004, 0]^T,$$
$$[0.0068, 0.7486, 0.4129, 0.0005]^T, [0.0001, 0, 0.0001, 0]^T,$$
$$[0.6096, 0.0007, 0.4818, 0.0003]^T, [0.0030, 0.0004, 0.4169, 0.0003]^T,$$
$$[0.3747, 0.3802, 0.0003, 0.0001]^T, [0.5190, 0.7249, 0.0006, 0.0003]^T,$$
$$[0.2273, 0.4783, 0.0050, 0.3437]^T, [0.7975, 0.3709, 0.0003, 0.0003]^T\}.$$

When the CCT value is 6500 K and $\sigma_e = 0.05$, the learned RGB LED constellation is given by

$$\mathcal{S} = \{[0.7608, 0.4065, 0.4893]^T, [0.0017, 0.89250.0007]^T, [0.1316, 0.6929, 0.5648]^T,$$
$$[0.2970, 0.0345, 0.5041]^T, [0.4081, 0.44850.0008]^T, [0.0157, 0.1529, 0.0006]^T,$$
$$[0.5897, 1.0000, 0.0011]^T, [0.8050, 0.01500.0081]^T\}.$$

When the CCT value is 6500 K and $\sigma_e = 0.05$, the learned QLED constellation is given by

$$\mathcal{S} = \{[0.7186, 0.0028, 0.0157, 0.0070]^T, [0.8293, 0.0001, 0.6149, 0.5176]^T,$$
$$[0.4796, 0.0008, 0.0201, 0.5431]^T, [0.3471, 0.3595, 0.4459, 0.8438]^T,$$
$$[0.9479, 0.1828, 0.6157, 0.0002]^T, [0.0090, 0.8577, 0.5678, 0.5106]^T,$$
$$[0.3727, 0.0005, 0.5658, 0.0003]^T, [0.7824, 0.6983, 0.0006, 0.0008]^T,$$
$$[0.0004, 0.8973, 0.3728, 0.0003]^T, [0.0005, 0.3275, 0.9653, 0.0004]^T,$$

$$[0.5599, 0.8934, 0.5910, 0.0007]^T, [0.5244, 0.3708, 1.0000, 0.2211]^T,$$
$$[0.0176, 0.0015, 0.6101, 0.4388]^T, [0.2279, 0.5091, 0.0006, 0.0003]^T,$$
$$[0.0008, 0.5224, 0.0010, 0.4837]^T, [0.5783, 0.7145, 0.0720, 0.5336]^T\}.$$

When the CCT value is 6500 K and $\sigma_e = 0.1$, the learned RGB LED constellation is given by

$$\mathcal{S} = \{[0.5711, 0.5967, 0.1341]^T, [0.0055, 0.4551, 0.5017]^T, [0.3849, 0.0041, 0.4838]^T,$$
$$[0.0004, 0.0005, 0.0011]^T, [0.3564, 0.1054, 0.0011]^T, [0.8139, 0.0051, 0.0016]^T,$$
$$[0.0332, 1.0000, 0.0034]^T, [0.0018, 0.4625, 0.0005]^T\}.$$

When the CCT value is 6500 K and $\sigma_e = 0.1$, the learned QLED constellation is given by

$$\mathcal{S} = \{[0.0008, 0.0104, 0.0022, 0.4302]^T, [0.8900, 0.0059, 0.2159, 0.0007]^T,$$
$$[0.0014, 0, 0.2232, 0.0002]^T, [0.1330, 0.5764, 0.0001, 0.4755]^T,$$
$$[0.5713, 0.0002, 0.8440, 0.0005]^T, [0.0002, 0.5641, 0.5924, 0.0002]^T,$$
$$[0.5657, 0.5580, 0.0001, 0.0004]^T, [0.0001, 0.0001, 0.7497, 0.0501]^T,$$
$$[0.0001, 0.4424, 0.5412, 0.5135]^T, [0.0001, 0.4871, 0.0001, 0.0004]^T,$$
$$[0.3732, 0.0001, 0.0001, 0.0002]^T, [0.6093, 0.5156, 0.4183, 0.3755]^T,$$
$$[0.3220, 0.0001, 0.4233, 0.5642]^T, [0.1701, 1.0000, 0.1774, 0.0009]^T,$$
$$[0.3262, 0.2097, 0.3494, 0.0014]^T, [0.5811, 0.0016, 0.0002, 0.4532]^T\}.$$

References

[1] A. Jovicic, J. Li, and T. Richardson, "Visible light communication: Opportunities, challenges and the path to market," *IEEE Commun. Mag.*, vol. 51, no. 12, pp. 26–32, Dec. 2013.

[2] H. Elgala, R. Mesleh, and H. Haas, "Indoor optical wireless communication: Potential and state-of-the-art," *IEEE Commun. Mag.*, vol. 49, no. 9, pp. 56–62, Sep. 2011.

[3] A. C. Boucouvalas, P. Chatzimisios, Z. Ghassemlooy, M. Uysal, and K. Yiannopoulos, "Standards for indoor optical wireless communications," *IEEE Commun. Mag.*, vol. 53, no. 3, pp. 24–31, Mar. 2015.

[4] P. H. Pathak, X. Feng, P. Hu, and P. Mohapatra, "Visible light communication, networking, and sensing: A survey, potential and challenges," *IEEE Commun. Surveys Tut.*, vol. 17, no. 4, pp. 2047–2077, Oct.–Dec. 2015.

[5] T. Komine and M. Nakagawa, "Fundamental analysis for visible-light communication system using LED lights," *IEEE Trans. Consum. Electron.*, vol. 50, no. 1, pp. 100–107, Feb. 2004.

[6] A.-M. Căilean and M. Dimian, "Current challenges for visible light communications usage in vehicle applications: A survey," *IEEE Commun. Surveys Tut.*, vol. 19, no. 4, pp. 2681–2703, Oct.–Dec. 2017.

[7] J. Grubor, S. Randel, K. Langer, and J. W. Walewski, "Broadband information broadcasting using LED-based interior lighting," *J. Lightw. Technol.*, vol. 26, no. 24, pp. 3883–3892, Dec. 2008.

[8] D. Karunatilaka, F. Zafar, V. Kalavally, and R. Parthiban, "LED based indoor visible light communications: State of the art," *IEEE Commun. Surveys Tut.*, vol. 17, no. 3, pp. 1649–1678, Jul.–Sep. 2015.

[9] Y. Wang, X. Huang, L. Tao, J. Shi, and N. Chi, "4.5-Gb/s RGB-LED based WDM visible light communication system employing CAP modulation and RLS based adaptive equalization," *Opt. Express*, vol. 23, no. 10, pp. 13 626–13 633, May 2015.

[10] G. Cossu, W. Ali, R. Corsini, and E. Ciaramella, "Gigabit-class optical wireless communication system at indoor distances (1.5/4 m)," *Opt. Express*, vol. 23, no. 12, pp. 15 700–15 705, Jun. 2015.

[11] Y. Wang, L. Tao, X. Huang, J. Shi, and N. Chi, "8-Gb/s RGBY LED-based WDM VLC system employing high-order CAP modulation and hybrid post equalizer," *IEEE Photon. J.*, vol. 7, no. 6, Dec. 2015, Art. no. 7904507.

[12] P. Das, Y. Park, and K.-D. Kim, "Performance of color-independent OFDM visible light communication based on color space," *Opt. Commun.*, vol. 324, pp. 264–268, 2014.

[13] D. A. Steigerwald *et al.*, "Illumination with solid state lighting technology," *IEEE J. Sel. Topics Quantum Electron.*, vol. 8, no. 2, pp. 310–320, Mar.–Apr. 2002.

[14] I. S. Association *et al.*, "IEEE standard for local and metropolitan area networks-part 15.7: Short-rang wireless optical communication using visible light," IEEE Standard 802, pp. 7–2011, 2011.

[15] R. J. Drost and B. M. Sadler, "Constellation design for color-shift keying using billiards algorithms," in *Proc. IEEE Globecom Workshops*, 2010, pp. 980–984.

[16] E. Monteiro and S. Hranilovic, "Constellation design for color-shift keying using interior point methods," in *Proc. IEEE Globecom Workshops*, 2012, pp. 1224–1228.
[17] X. Liang, M. Yuan, J. Wang, Z. Ding, M. Jiang, and C. Zhao, "Constellation design enhancement for color-shift keying modulation of quadrichromatic LEDs in visible light communications," *J. Lightw. Technol.*, vol. 35, no. 17, pp. 3650–3663, Sep. 2017.
[18] A. N. ANSLG, "C78.377–2008: Specifications for the chromaticity of solid state lighting products," Washington, DC, USA: ANSI, American National Standard Institute, 2008.
[19] J.-M. Dong, Y.-J. Zhu, and Z.-G. Sun, "Adaptive multi-color shift keying constellation design for visible light communications considering lighting requirement," *Opt. Commun.*, vol. 430, pp. 293–298, 2019.
[20] T. OShea and J. Hoydis, "An introduction to deep learning for the physical layer," *IEEE Trans. Cogn. Commun. Netw.*, vol. 3, no. 4, pp. 563–575, Dec. 2017.
[21] H. He, S. Jin, C.-K. Wen, F. Gao, G. Y. Li, and Z. Xu, "Model-driven deep learning for physical layer communications," *IEEE Wireless Commun.*, vol. 26, no. 5, pp. 77–83, Oct. 2019.
[22] H. Lee, I. Lee, and S. H. Lee, "Deep learning based transceiver design for multi-colored VLC systems," *Opt. Express*, vol. 26, no. 5, pp. 6222–6238, 2018.
[23] E. Monteiro and S. Hranilovic, "Design and implementation of color-shift keying for visible light communications," *J. Lightw. Technol.*, vol. 32, no. 10, pp. 2053–2060, May 2014.
[24] J. R. Barry, *Wireless Infrared Communications*. Berlin, Germany: Springer, 2012, vol. 280.
[25] B. E. Saleh and M. C. Teich, *Fundamentals of Photonics*. Hoboken, NJ, USA: Wiley, 2019.
[26] Y.-Y. Zhang, "Intrinsic robustness of MISO visible light communications: Partial CSIT can be as useful as perfect one," *IEEE Trans. Commun.*, vol. 67, no. 2, pp. 1297–1312, Feb. 2019.
[27] S. Karp, R. M. Gagliardi, S. E. Moran, and L. B. Stotts, *Optical Channels: Fibers, Clouds, Water, and The Atmosphere*. Berlin, Germany: Springer, 2013.
[28] D. Marcuse, "Calculation of bit-error probability for a lightwave system with optical amplifiers and post-detection Gaussian noise," *J. Lightw. Technol.*, vol. 9, no. 4, pp. 505–513, Apr. 1991.
[29] J. R. Barry, J. M. Kahn, W. J. Krause, E. A. Lee, and D. G. Messerschmitt, "Simulation of multipath impulse response for indoor wireless optical channels," *IEEE J. Sel. Areas Commun.*, vol. 11, no. 3, pp. 367–379, Apr. 1993.
[30] L. Zeng *et al.*, "High data rate multiple input multiple output (MIMO) optical wireless communications using white LED lighting," *IEEE J. Sel. Areas Commun.*, vol. 27, no. 9, pp. 1654–1662, Dec. 2009.
[31] Q. Gao, R. Wang, Z. Xu, and Y. Hua, "DC-informative joint color-frequency modulation for visible light communications," *J. Lightw. Technol.*, vol. 33, no. 11, pp. 2181–2188, Jun. 2015.
[32] H. Ma, A. Mostafa, L. Lampe, and S. Hranilovic, "Coordinated beamforming for downlink visible light communication networks," *IEEE Trans. Commun.*, vol. 66, no. 8, pp. 3571–3582, Aug. 2018.
[33] H. Marshoud, D. Dawoud, V. M. Kapinas, G. K. Karagiannidis, S. Muhaidat, and B. Sharif, "MU-MIMO precoding for VLC with imperfect CSI," in *Proc. IEEE 4th Int. Workshop Opt. Wireless Commun.*, 2015, pp. 93–97.
[34] T. Smith and J. Guild, "The CIE colorimetric standards and their use," *Trans. Opt. Soc.*, vol. 33, no. 3, pp. 73–134, 1931.
[35] G. Wyszecki and W. S. Stiles, *Color Science*. New York, NY, USA: Wiley, 1982, vol. 8.
[36] T. V. Pham, H. Le-Minh, and A. T. Pham, "Multi-user visible light communication broadcast channels with zero-forcing precoding," *IEEE Trans. Commun.*, vol. 65, no. 6, pp. 2509–2521, Jun. 2017.
[37] E. Monteiro and S. Hranilovic, "Design and implementation of color-shift keying for visible light communications," *J. Lightw. Technol.*, vol. 32, no. 10, pp. 2053–2060, May 2014.
[38] M. Soltani, W. Fatnassi, A. Aboutaleb, Z. Rezki, A. Bhuyan, and P. Titus, "Autoencoder-based optical wireless communications systems," in *Proc. IEEE Globecom Workshops (GC Wkshps)*, 2018, pp. 1–6.
[39] D.-A. Clevert, T. Unterthiner, and S. Hochreiter, "Fast and accurate deep network learning by exponential linear units (elus)," 2015, *arXiv:1511.07289*.
[40] D. P. Kingma and J. Ba, "Adam: A method for stochastic optimization," 2014, *arXiv:1412.6980*.
[41] M. Matsumoto and T. Nishimura, "Mersenne twister: A 623-dimensionally equidistributed uniform pseudo-random number generator," *ACM Trans. Model. Comput. Simul.*, vol. 8, no. 1, pp. 3–30, 1998.
[42] M. Abadi *et al.*, "Tensorflow: Large-scale machine learning on heterogeneous distributed systems," 2016, *arXiv:1603.04467*.
[43] A. Wiesel, Y. C. Eldar, and A. Beck, "Maximum likelihood estimation in linear models with a Gaussian model matrix," *IEEE Signal Process. Lett.*, vol. 13, no. 5, pp. 292–295, May 2006.
[44] A. Wiesel, Y. C. Eldar, and A. Yeredor, "Linear regression with Gaussian model uncertainty: Algorithms and bounds," *IEEE Trans. Signal Process.*, vol. 56, no. 6, pp. 2194–2205, Jun. 2008.